

# Electronic Supporting Information

## **A light-fueled dissipative aggregation-induced emission system for time-dependent information encryption**

Caixia Yang,<sup>abc</sup> Hangxiang Xiao,<sup>c</sup> Zichen Luo,<sup>c</sup> Li Tang,<sup>a</sup> Bailin Dai,<sup>a</sup> Ningbo Zhou,<sup>cd</sup> Enxiang Liang,<sup>\*cd</sup> Guoxiang Wang,<sup>cd</sup> and Jianxin Tang<sup>\*a</sup>

<sup>a</sup>Hunan Key Laboratory of Biomedical Nanomaterials and Devices, College of Life Sciences and Chemistry, Hunan University of Technology, Zhuzhou, 412007, PR China.

<sup>b</sup>College of Packaging and Material Engineering, Hunan University of Technology, Zhuzhou 412007, PR China

<sup>c</sup>College of Chemistry and Chemical Engineering, Hunan Institute of Science and Technology Yueyang, Hunan Province 414006, PR China.

<sup>d</sup>Key Laboratory of Hunan Province for Advanced Carbon-based Functional Materials, School of Chemistry and Chemical Engineering, Hunan Institute of Science and Technology, Yueyang, 414006, PR China

Email: exliang@hnist.edu.cn, wanggxwzl@163.com, jxtang0733@163.com

## 1. Materials

Benzophenone (99.5%), zinc powder (99.9%) fuming nitric acid, raney Ni, tetrahydrofuran (THF) and 1,3-propanesultone were obtained from Adamas Reagent Co., Ltd (Shanghai, China). Acetic acid (glacial), 2,3,3-trimethyl-3H-indole, salicylaldehyde, dichloromethane and ethyl acetate were obtained from Tansoole (Shanghai, China). THF was purified by distillation from sodium benzophenone under nitrogen immediately prior to use. All chemicals were used without purification unless otherwise noted.

## 2. Characterisations

<sup>1</sup>H NMR spectra were recorded on a 400 MHz Bruker Avance-400 NMR spectrometer. Mass spectral data were measured with XEVO G2-S QTOF (ESI) (Waters, USA). UV spectra were measured on a Milton Roy Spectronic 3000 Array spectrophotometer and the FL spectra were recorded on a Perkin-Elmer LS 55 spectrofluorometer with a Xenon discharge lamp excitation. Samples in aqueous solution for absorption and emission measurements were carried out in 1 cm × 1 cm quartz cuvettes. The absolute fluorescence quantum yield ( $\Phi$ ) was measured using an Edinburgh Instrument FLS920 steady state spectrometer. The TEM photographs were obtained using a transmission electron microscope (Hitachi H7650, Tokyo, Japan). Average hydrodynamic diameter ( $D_h$ ) and Zeta potential of aggregates were determined using a dynamic light scattering (DLS) (Zetasizer Nano ZS, Malvern Instrument Ltd., UK) instrument. The pH values were measured by the PHSJ-3F pH meter (Shanghai REX, China). Pictures were obtained by a Canon digital camera. Millipore water was used to prepare all aqueous solutions. All experiments were performed at room temperature (~25 °C) unless otherwise specified.

## 3. Calculations

The geometries of the photoacid (SMEH or ASP) and TPE4N<sup>4+</sup> at the ground state were fully optimized by means of the B3LYP/6-31G(d) level method. Density functional theory (DFT) calculations at the B3LYP/6-31G(d) level were performed in the Gaussian 09 package. RDG surface was analyzed from the information of the calculation result and generated by Multiwfn 3.6. Based on the optimized geometries, the binding energies (BE) between photoacid (SMEH or ASP) and TPE4N<sup>4+</sup> were calculated by the following formula:

$$BE = (E_P + E_T) - E_{Total} \quad (1)$$

Where  $E_{Total}$  is the total energy of photoacid-TPE4N<sup>4+</sup> system,  $E_T$  is the total energy of water,  $E_P$  is

the energy of TPE4N<sup>4+</sup>.

#### 4. Synthesis

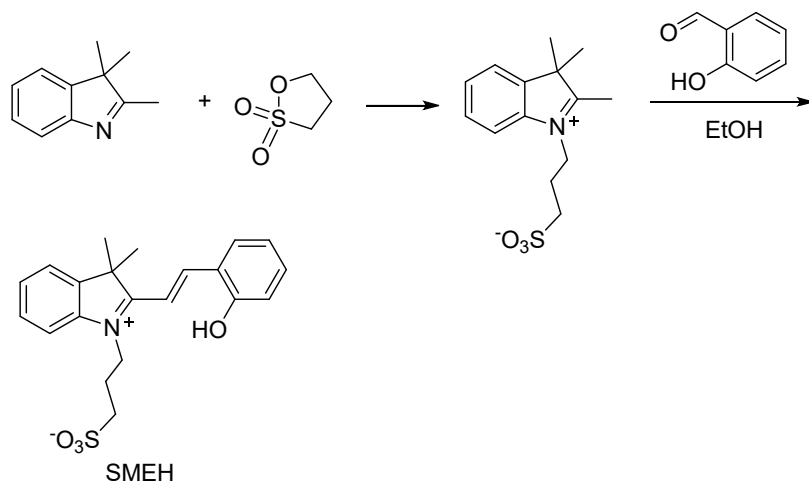


Fig.S1 The synthetic scheme of SMEH

##### 4.1 Synthesis of TPE4N<sup>4+</sup>

TPE4N<sup>4+</sup> were synthesized according to the reported method<sup>[1]</sup>.

##### 4.2 Synthesis of SMEH

SMEH was synthesized according to literature<sup>[2]</sup>. A solution of 1,3-propanesultone (1.65 mL, 2.30 g, 18.8 mmol, 1.00 eq.) and 2,3,3-trimethyl-3H-indole (3.02 mL, 3.00 g, 18.8 mmol, 1.00 eq.) in toluene (100 mL) was heated to 135 °C for 2.5 days. After letting the solution cool to room temperature, the purple precipitate was collected by vacuum filtration and washed with petroleum ether (ca. 15 mL, 40/60). The precipitate was dried in vacuo for ca. 24 h and gave a purple solid as 3-(2,3,3-trimethyl-3H-indol-1-ium-1-yl)propane-1-sulfonate (3.52 g, 12.5 mmol, 66%) which was used in the consecutive reaction without further purification. Salicylaldehyde (41.7 μL, 47.7 mg, 391 μmol, 1.44 eq.) was added to a solution of the substituted indolinium (100 mg, 271 μmol, 1.00 eq.) in anhydrous ethanol (136 mM, 2.00 mL). The reaction mixture was heated to 95 °C for 17 h and let cool down to room temperature. The resulting orange precipitate SMEH was collected by vacuum filtration, washed with ethanol (ca. 2 mL) and dried in vacuo giving an orange powder (70.6 mg, 183 μmol, 67.8%). The structure was determined by <sup>1</sup>H-NMR, <sup>13</sup>C-NMR and HRMS. <sup>1</sup>H NMR (400 MHz, DMSO-d<sub>6</sub>): δ 11.07 (s, 1H, OH), 8.59 (d, J = 16.5 Hz, 1H, H<sup>g</sup>), 8.30 (d, J = 7.7 Hz, 1H, H<sup>c</sup>), 8.02 (d, J = 7.6 Hz, 1H, H<sup>p</sup>), 7.87 (d, J = 7.4 Hz, 2H, H<sup>m+h</sup>), 7.63 (m, 2H, H<sup>n+o</sup>), 7.48 (t, J = 7.6 Hz, 1H, H<sup>c</sup>), 7.04 (d, J = 8.3 Hz, 1H, H<sup>b</sup>), 6.99 (d, J = 7.4 Hz, 2H, H<sup>d</sup>), 4.83 (m, 2H, H<sup>r</sup>), 2.68 (t, J = 6.4 Hz, 2H, H<sup>t</sup>), 2.19 (p, J = 7.1 Hz, 2H, H<sup>s</sup>), 1.78 (s, 6H, H<sup>k</sup>).

<sup>13</sup>C NMR (400 MHz, DMSO-d<sub>6</sub>) δ 182.30 (C<sup>i</sup>), 159.38 (C<sup>a</sup>), 149.30 (C<sup>g</sup>), 143.88 (C<sup>l</sup>), 141.17 (C<sup>q</sup>),

135.95(C<sup>c</sup>), 130.24 (C<sup>e</sup>), 129.62 (C<sup>n+o</sup>), 129.48 (C<sup>n+o</sup>), 123.46 (C<sup>m</sup>), 121.81 (C<sup>f</sup>), 120.53 (C<sup>d</sup>),  
 117.22 (C<sup>b</sup>), 115.57 (C<sup>p</sup>), 111.74 (C<sup>h</sup>), 52.55 (C<sup>j</sup>), 48.71 (C<sup>l</sup>), 47.65 (C<sup>r</sup>), 27.25 (C<sup>k</sup>), 24.84(C<sup>s</sup>).

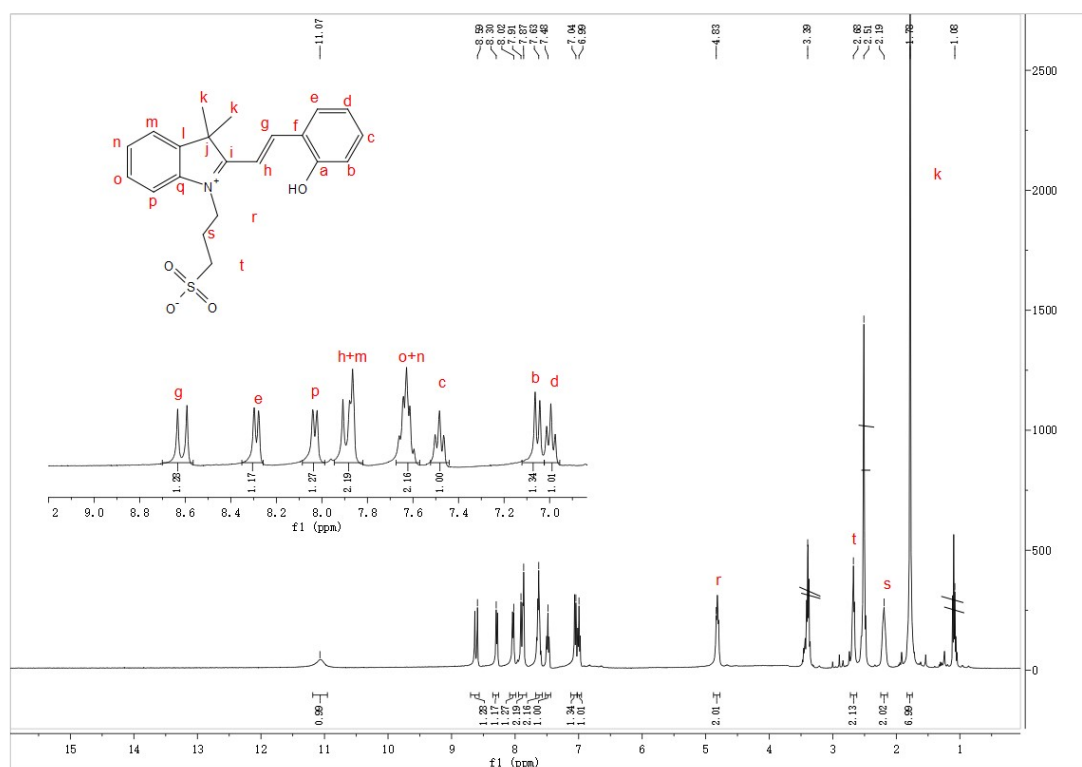


Fig.S2 <sup>1</sup>H NMR of SMEH

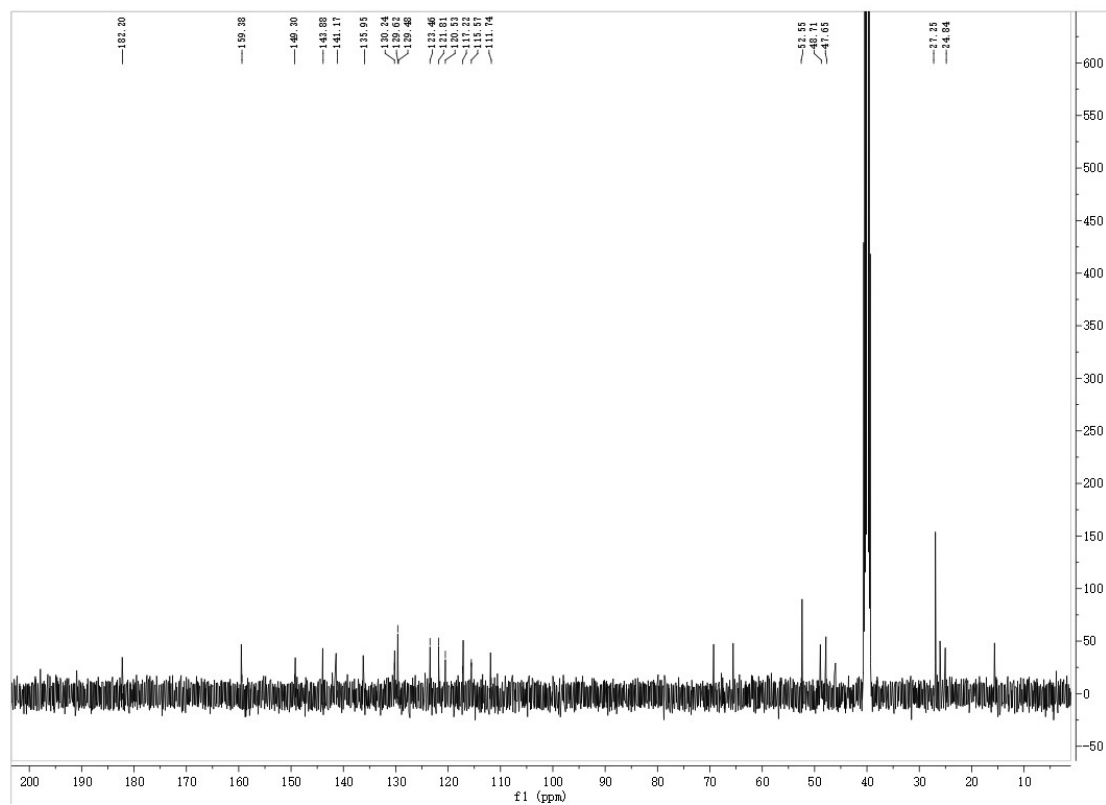


Fig.S3 <sup>13</sup>C NMR of SMEH

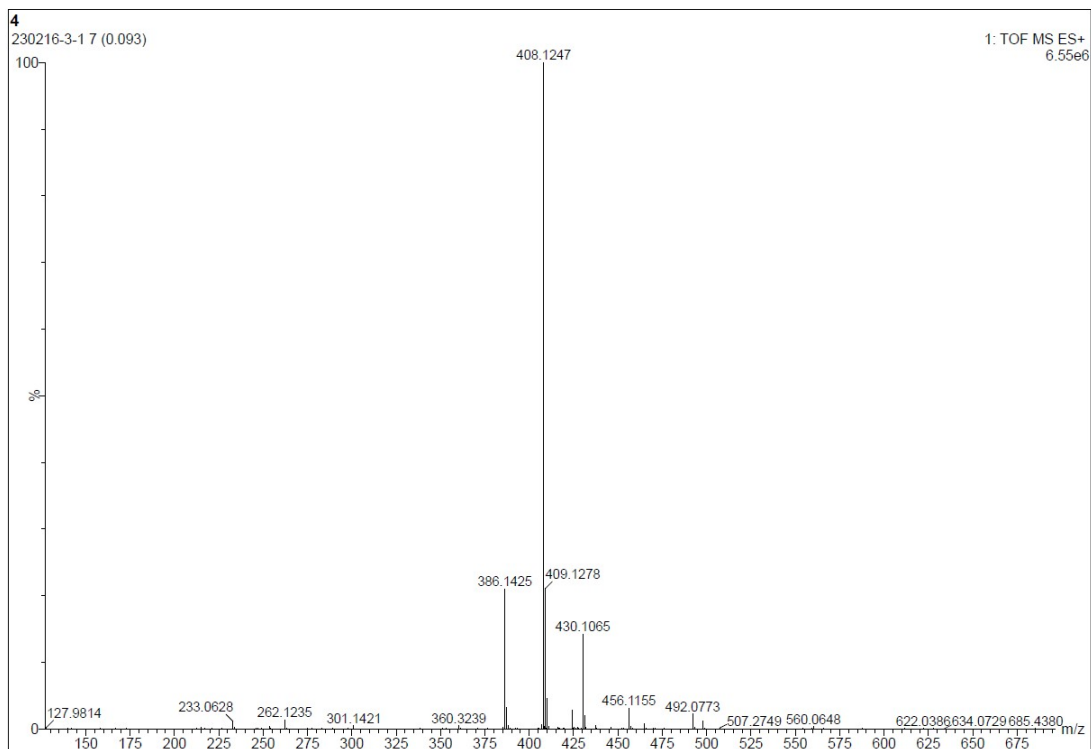


Fig.S4 MS spectra of SMEH

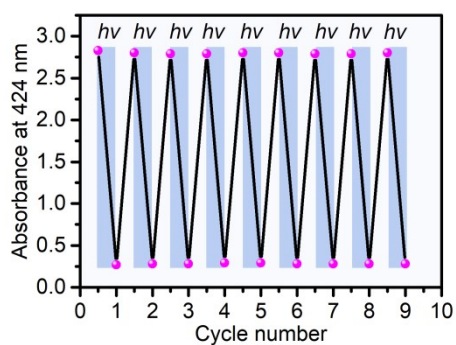


Fig.S5 Cycles of absorbance at 424 nm of SMEH before and after irradiation

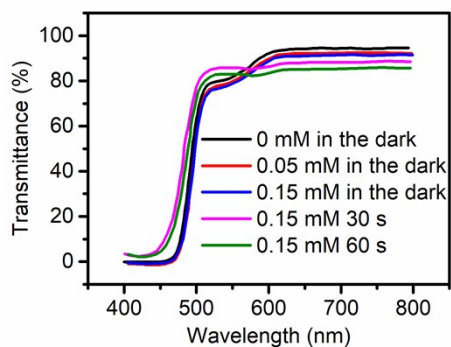


Fig.S6 Transmittance at 650 nm of SMEH-TPE4N<sup>4+</sup> in aqueous solution before and after irradiation. [SMEH] = 0.15 mM, the concentration of TPE4N<sup>4+</sup> vary from 0 to 0.15 Mm

### Determination of the preferable assembly concentration of ASP-TPE4N<sup>4+</sup> by optical transmittance<sup>[3]</sup> (Fig.S7 and S8)

The critical aggregation concentration (CAC) of ASP (represented by the initial concentration of SMEH) in TPE4N<sup>4+</sup> was determined by investigating the optical transmittance with fixing the concentration of TPE4N<sup>4+</sup> (0.15 mM) and increasing the concentration of SMEH from 0.02 to 0.18 mM right after 420 nm irradiation for 10 min (Fig. S7). The optical transmittance at 650 nm showed different linear variation with the appearance of an inflection point at 0.082 mM, which indicated the induced CAC of SMEH in presence of TPE4N<sup>4+</sup> (5 mM) was 0.082 mM. While ranging the concentration of TPE4N<sup>4+</sup> from 0.03 to 0.21 mM in SMEH solution (0.15 mM), the optical transmittance at 650 nm gradually decreased before 0.15 mM and then sharply recovered after 420 nm irradiation (Fig.S8), which indicated the preferable mixing ratio of SMEH-TPE4N<sup>4+</sup> was measured as 0.15 mM SMEH/0.15 mM TPE4N<sup>4+</sup>.

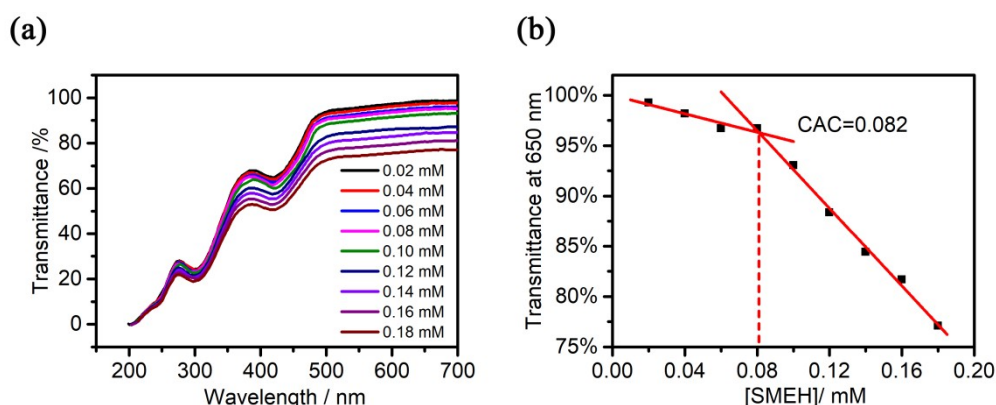


Fig.S7 Transmittance of TPE4N<sup>4+</sup>(0.15 mM) in varying concentration of SMEH from 0.02 mM to 0.18 mM right after irradiation with 420 nm light for 10 min. (b) Transmittance at 650 nm of spectrum (a) and the CAC fitting graph.

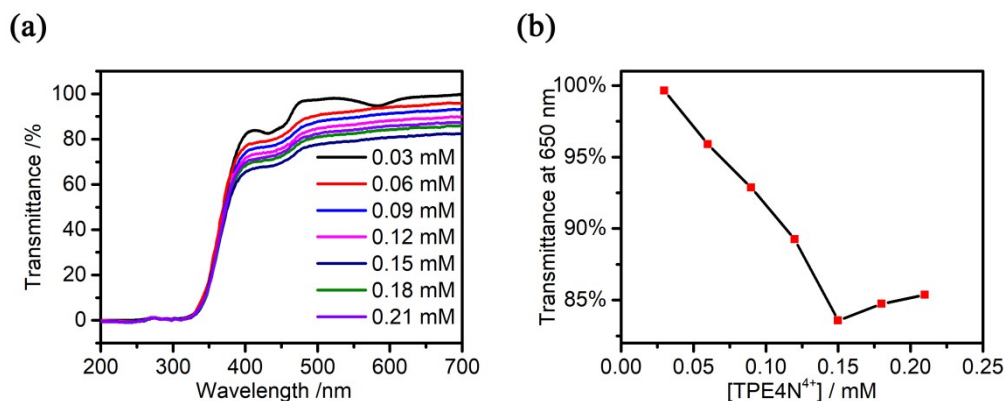


Fig.S8 (a) Transmittance of SMEH (0.15 mM) in varying concentration of TPE4N<sup>4+</sup> (0.03 mM-

0.21 mM) right after 420 nm irradiation for 10 min. (b) Transmittance at 650 nm of spectrum (a).

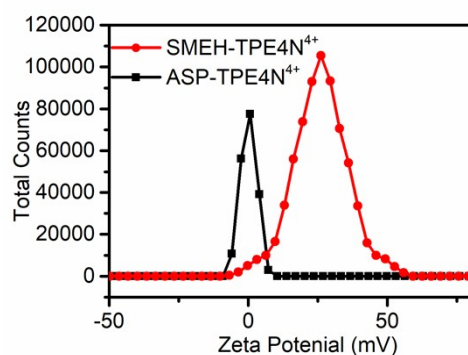


Fig.S9 Zeta potential of SMEH-TPE4N<sup>4+</sup> and ASP-TPE4N<sup>4+</sup>

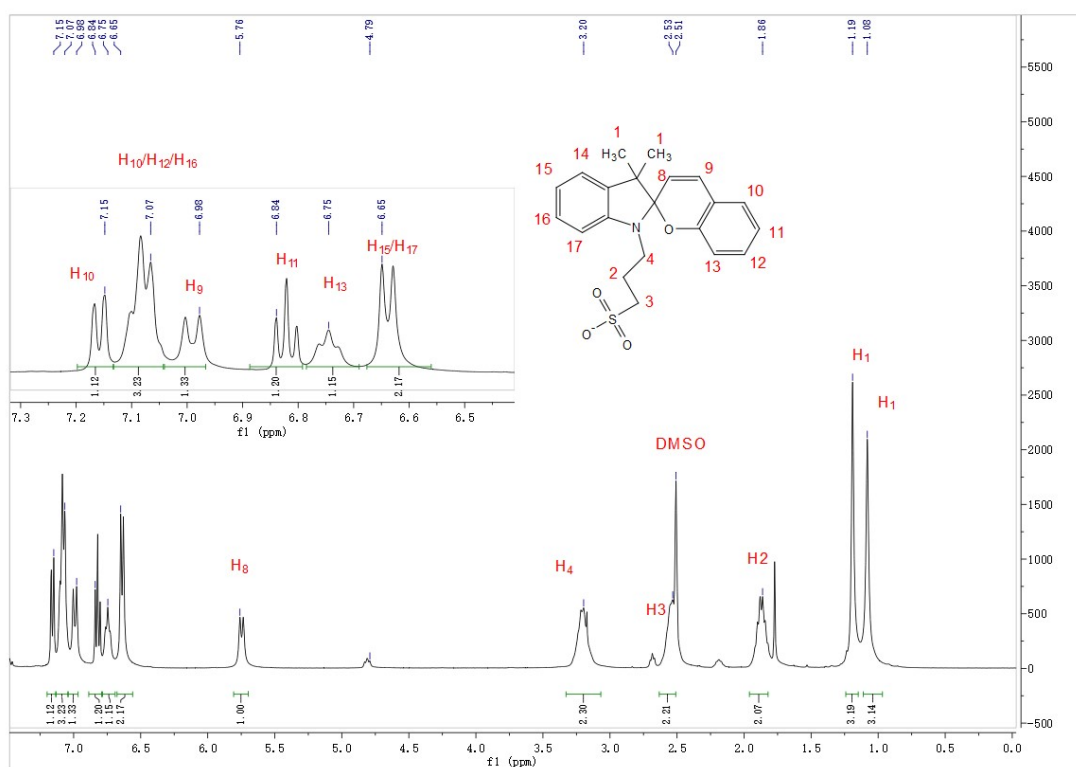


Fig.S10 <sup>1</sup>H NMR of ASP in DMSO-d<sub>6</sub>

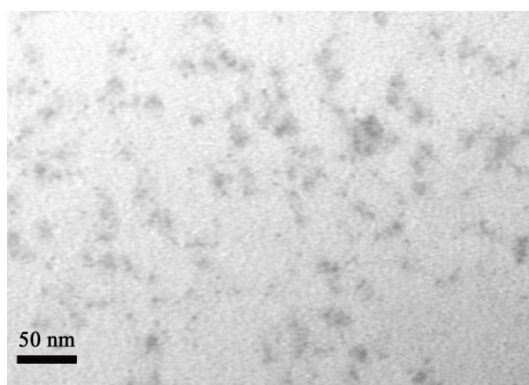


Fig.S11 TEM image of SMEH (0.15 mM)-TPE4N<sup>4+</sup> (0.15 mM) in the dark.

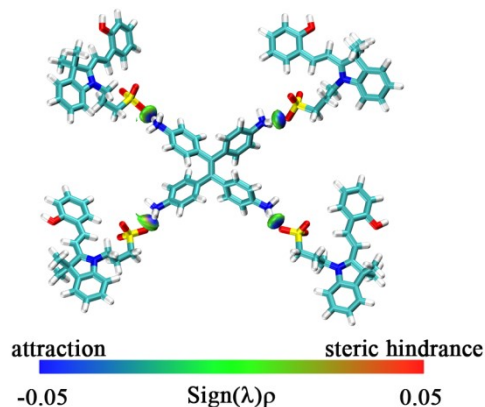


Fig.S12 RDG analysis on optimized structures of TPE4N<sup>4+</sup> and SMEH units.

Tab. S1 Binding energy for SMEH-TPE4N<sup>4+</sup> system and ASP-TPE4N<sup>4+</sup> system

System	$E_{\text{Total}}$ (Hartree)	$E_{\text{P}}$ (Hartree)	$E_{\text{T}}$ (Hartree)	BE (ev)
SMEH-TPE4N <sup>4+</sup> system	-7498.35	-6272.09	-1226.19	1.9
ASP-TPE4N <sup>4+</sup> system	-7496.49	-6270.21	-1226.19	2.5

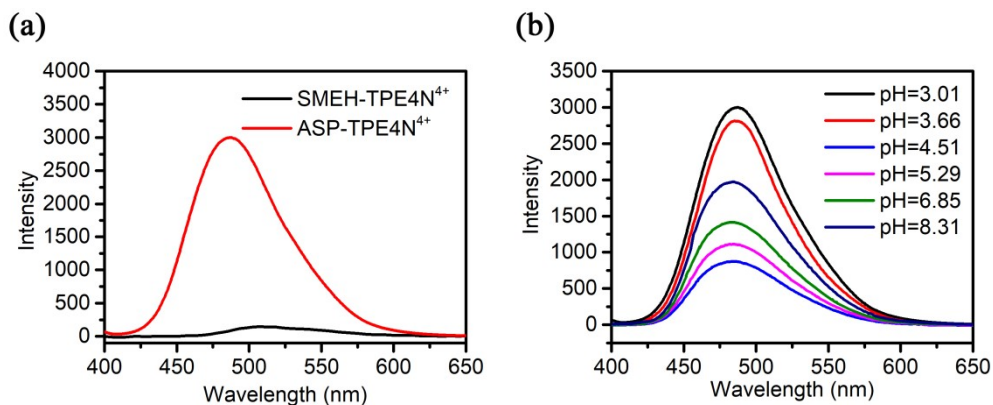


Fig.S13 (a) Fluorescence emission of SMEH-TPE4N<sup>4+</sup> and ASP-TPE4N<sup>4+</sup> aqueous solution. (b) PL spectra of ASP-TPE4N<sup>4+</sup> in aqueous solutions with different pH values

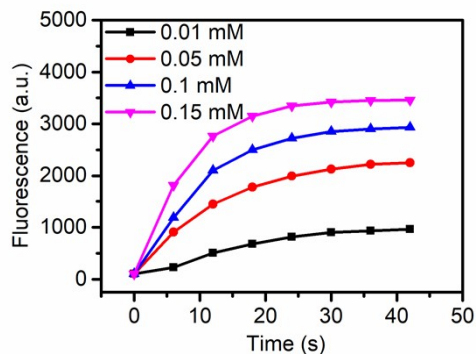


Fig.S14 Changes in fluorescence at 485 nm of SMEH-TPE4N<sup>4+</sup> aqueous solution upon 420 nm



irradiation

Tab.S2 First order kinetic parameters of SMEH-TPE4N<sup>4+</sup> upon 420 nm irradiation

Sample name	$k$	$\tau_{1/2}$	R-square
SMEH (x mM)-TPE4N <sup>4+</sup> (0.15 mM)			
0.01 : 0.15	0.0717	9.66	0.98868
0.05 : 0.15	0.09595	7.22	0.99029
0.1 : 0.15	0.10972	6.31	0.99799
0.15 : 0.15	0.14724	4.71	0.99797

Note:  $k$  is the kinetic rate constant.  $\tau_{1/2}$  is the half-life ( $\tau_{1/2}=\ln 2/k$ ).

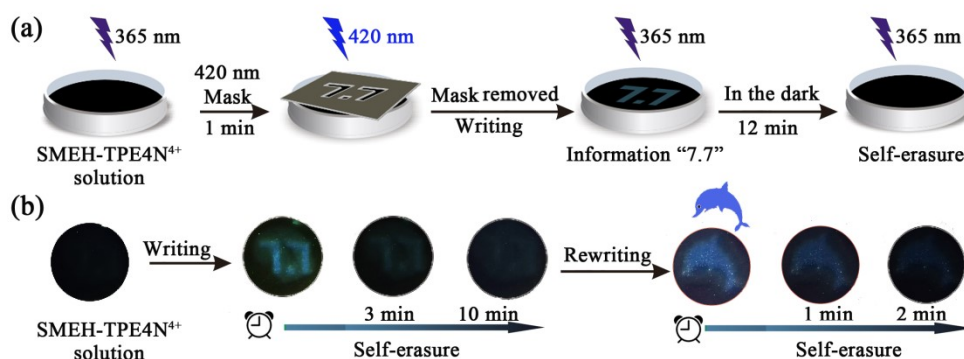


Fig.S15 (a) Schematic representation of the 420 nm light writing and 365 nm emitting the patterns in the petri dish. (b) Photo of writing pattern and self-erasing process

## Reference

- [1] E. Liang, F. Su, Y. Liang, G. Wang, W. Xu, S. Li, C. Yang, J. Tang and N. Zhou, *Chem. Commun.*, 2020, **56**, 15169-15172.
- [2] C. Berton, D. M. Busiello, S. Zamuner, E. Solari, R. Scopelliti, F. Fadaei-Tirani, K. Severin and C. Pezzato, *Chem. Sci.*, 2020, **11**, 8457-8468.
- [3] X. Chen, Y. Chen, X. Hou, X. Wu, B. Gu, Y. Liu, *ACS Appl.Mater. Interfaces* 2018, 10, 24987-24992.